Absolute total and partial cross sections for ionization of nucleobases by proton impact in the Bragg peak velocity range

J. Tabet, S. Eden,[*] S. Feil, H. Abdoul-Carime, B. Farizon, M. Farizon, S. Ouaskit,[†] and T. D. Märk[‡]

Université de Lyon, F-69003, Lyon, France Université Lyon 1, Villeurbanne, France, and
CNRS/IN2P3, UMR5822, Institut de Physique Nucléaire de Lyon, F-69622, Villeurbanne, France

We present experimental results for proton ionization of nucleobases (adenine, cytosine, thymine, and uracil) based on an event-by-event analysis of the different ions produced combined with an absolute target density determination. We are able to disentangle in detail the various proton ionization channels from mass-analyzed product ion signals in coincidence with the charge-analyzed projectile. In addition we are able to determine a complete set of cross sections for the ionization of these molecular targets by 20–150 keV protons including the total and partial cross sections and the direct-ionization and electron-capture cross sections.

PACS number(s): 34.70.+e, 82.30.Fi, 82.39.Pj

I. INTRODUCTION

Besides their fundamental importance in collisions [1], molecular ionization and dissociation processes are of great interest in diverse areas of science ranging from plasma physics to radiation damage in biological tissues [2]. Today it is recognized that radiation damage in biomolecules, notably the formation of DNA strand breaks, is not only the result of a single interaction of the primary ionization projectile with the molecules involved, but also due to the simultaneous and consecutive action of the primary and secondary species [3]. A detailed knowledge of the ionization and dissociation processes involved including the various cross sections is a must for a full understanding of radiation damage on a microscopic level (see, e.g., [4,5]).

This has led recently to an increased number of investigations on the interactions of the various primary and secondary species with DNA and its constituents. Gas- and solid-phase experiments have been carried out with isolated basic constituents of DNA (i.e., the nucleobases, phosphate, sugar, and water subunits) involving target molecules and molecular compounds of increasing complexity. Many of these seminal studies have been devoted to the interaction of low-energy electrons (e.g., see [6–13]). This work has led to major advances in understanding the role of the secondary low-energy electrons in radiobiology with potential applications in radiotherapy [14].

In contrast to studies of electron-induced processes, investigations concerning proton (or heavier ions, for example, see [15,16]) interactions with DNA and its constituents are rather scarce, and a number of details have not yet been investigated. This is particularly intriguing as the interaction of protons in the keV energy range with building blocks of DNA is of great biological relevance in view of the ever increasing number of proton therapy facilities using MeV proton irradiation [17]. When these protons enter the tissue, they are decelerated reaching Bragg peak energies. These tumor treatments exploit the Bragg peak maximum and its volume selectivity based on the intricate interplay of the various primary and secondary interaction processes. Despite being such a promising tool for cancer treatment, most proton interaction studies reported so far either have been restricted to a specific type of cross section or have involved targets consisting of atoms or small (atmospheric) molecules. Although numerous total electron-capture cross sections are available for proton interactions with gases [18–20], only recently have complete sets of ionization cross sections (including the total and partial cross sections for direct ionization and electron capture) been reported for protons (or hydrogen) collisions with condensable molecular targets such as H_2O [21–23]. In 2003, Coupier *et al.* [24] reported the first mass spectrum for the direct ionization of uracil with 20–150 keV protons in comparison with electron impact ionization. Moretto-Capelle and Le Padellec [25] followed this up with an electron spectroscopy study obtaining double differential cross sections showing preferential emission of low-energy electrons for 25–100 keV proton impact on gas-phase uracil. Alvarado *et al.* [26] recently used a new experimental approach to directly measure the amount of internal energy present in deoxyribose dications after keV proton collisions with gas-phase molecules. Finally, Le Padellec *et al.* [27] reported mass spectra for 100 keV proton impact ionization of gas-phase cytosine, thymine, and uracil.

In this publication, we report on the application of an experimental setup that allows us, on an event-by-event basis, to analyze in great detail proton impact ionization of nucleobases (adenine, cytosine, thymine, and uracil) and to measure absolute partial and total single ionization cross sections as a function of the charge state of the projectile after the ionization event. Mass-analyzed product ions were detected (providing fragmentation pattern data) in coincidence with the charge-analyzed projectile after the ionizing collision, i.e., H^+ detection after direct ionization (DI), neutral $H°$ detection after single electron capture (EC), or H^- detection after double

---

[*]Current address: Department of Physics and Astronomy, The Open University (OU), Walton Hall, Milton Keynes, MK76 AA, UK.

[†]Current address: Laboratoire de Physique de la Matière Condensée, Unité Associée au CNRST (URAC 10), Faculté des Sciences Ben M'sik, B.P. 7955, Casablanca, Morocco.

[‡]Current address: Institut für Ionenphysik und Angewandte Physik, Leopold Franzens Universitat, Technikerstrasse 25, A-6020 Innsbruck, Austria.

electron capture [28,29]. The present study became possible by the development of a temperature-controlled Knudsen-type molecular beam source with absolutely characterized target thickness. We are thus able to disentangle the various reaction channels in proton ionization of nucleobases and provide in addition absolute ionization and dissociation cross sections that are "differential" in terms of the projectile state. Thus, absolute cross sections for proton ionization become available for targets which exist in the solid state (powder) under normal atmospheric conditions. Here, we report on results involving positive product ion formation: direct ionization and single-electron-capture events.

II. EXPERIMENT

The experimental apparatus is shown in Fig. 1. It consists essentially of five parts (partially shown in Fig. 1): First, pure molecular hydrogen is ionized in a standard rf-discharge source [30]. Second, ions from the source are accelerated to 20–150 keV with an energy resolution $\Delta E/E$ of 0.01 [30]. Third, the primary magnetic sector field shown in Fig. 1 is used as a mass selector to produce a pure beam of protons which is followed by a parallel plate deflector allowing detection of the primary ion beam. Fourth, the proton beam intersects a perpendicular effusive jet of sublimated nucleobase molecules and the cross-beam interaction region is coupled to a time-of-flight mass spectrometer. The effusive neutral target beam jet is produced by sublimating nucleobase powder samples (purchased from Sigma-Aldrich, minimum purity 99%) in a temperature-controlled Knudsen-type oven with a capillary exit of 1 mm diameter. The target thickness and distribution have been determined by combining mass measurements of the condensed nucleobases on a liquid-nitrogen-cooled aluminum plate mounted above the capillary exit, with deposition patterns measured by optical interference analysis and calculated angular distribution profiles using Troitskii's vapor flow model [31,32]. We have ascertained that no thermal decomposition takes place in the temperature range 390–500 K used in the present experiments. Finally, the projectiles pass through a sec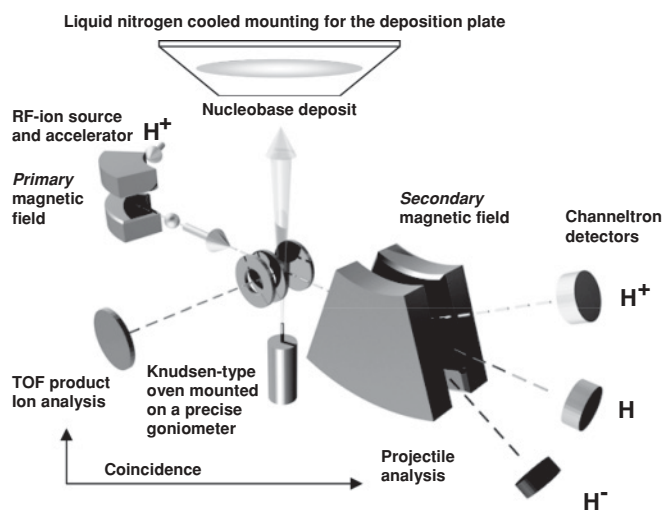ond (sector field type magnetic) mass selector combined with a multidetector device using Channeltron detectors that are located at different positions at the exit of the magnetic analyzer, thus giving us information about the final charge state of the projectile (i.e., protons will be deflected and neutralized protons will be undeflected by the magnet). We have checked single-collision conditions by changing the densities of both beams. Then, the nucleobase parent and fragment ions produced are extracted perpendicularly to the direction of both, the projectile and the target beam, and then mass-to-charge analyzed in a time-of-flight analyzer in coincidence with the projectile signal at the multidetector device. This allows us to record simultaneously the charged product ions produced in the target region and in coincidence for each single-collision event the nature of the projectile (either H^+ or after electron capture neutral H) after the ionizing collision.

III. RESULTS AND DISCUSSION

As examples, Fig. 2 shows mass spectra for single-ion-production events in 80 and 42 keV proton collisions with gas-phase uracil. Each mass spectrum was constructed after the interaction of about 10^7–10^8 protons with the target beam producing about 10^4 product ions. Having applied our coincidence technique, we can (in contrast to earlier studies with protons

FIG. 1. Schematic diagram of the experimental system.
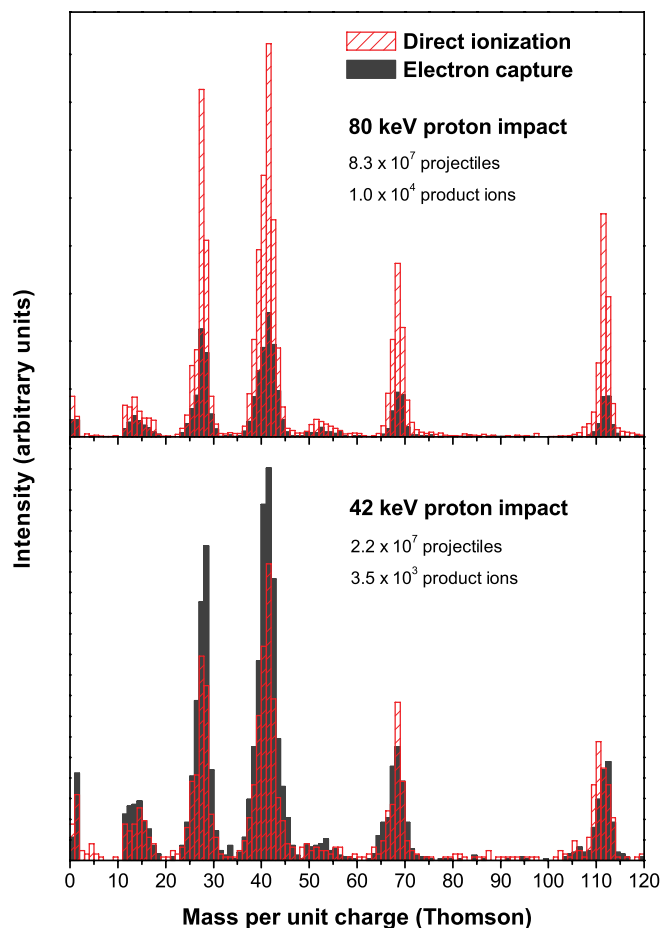

FIG. 2. (Color online) Mass spectra for direct ionization and electron capture in 80 and 42 keV proton collisions with gas-phase uracil.

TABLE I. Branching ratios for selected ionization and dissociative ionization processes in 27–150 keV proton collisions with gas-phase nucleobase molecules.

	Branching ratio (%)[a]						
	Uracil				Cytosine	Adenine	Thymine
	27 keV	42 keV	80 keV	150 keV	80 keV	80 keV	80 keV
Electron capture (EC)	57.0	47.6	25.4	8.5	27.6	27.1	26.6
[Total ionization (EC + DI)]	±9.2	±8.5	±2.0	±2.0	±4.0	±4.0	±4.0
Fragment ion production by EC	89.8	90.5	90.4	88.6	91.9	91.6	94.1
[Total EC (fragment + parent ions)]	±0.7	±0.7	±0.7	±1.8	±0.5	±1.0	±0.4
Fragment ion production by DI	94.5	84.0	84.5	84.7	84.9	82.8	89.3
[Total DI (fragment + parent ions)]	±2.7	±3.6	±0.7	±0.8	±0.6	±1.6	±0.8

[a]The errors are generally greater for the branching ratios involving DI detection at 42 keV because the Channeltron signal threshold had to be set quite close to the noise level.

[24,27] and multiply charged ions [33]) distinguish between ions produced by direct ionization (DI) of uracil via $U + H^+ \rightarrow$ ions $+ H^+$ and ions produced via electron capture (EC) via $U + H^+ \rightarrow$ ions $+ H$ [34,35]. Besides parent ion production, strong fragmentation is observed for both EC and DI leading to the appearance of five groups of fragment ions with neighboring mass numbers. In both ionization processes, the total fragment ion abundance is clearly much larger than the respective parent ion abundance. Table I includes uracil fragmentation branching ratios (fragment ion production to total ion production) for EC and DI at selected energies in the range 27–150 keV. In general, the total fragment ion abundance is larger for the electron-capture reaction, which can be rationalized by arguing that in the case of the direct-ionization mechanism, less energy is transferred to the molecular system. Moreover, the fragmentation ratio (sum of fragment ions divided by parent ion intensities) is for both cases rather independent of the kinetic energy (Table I); only at energies below about 40 keV does the fragmentation ratio increase strongly in the case of direct ionization (due to a strong decrease of the parent ion abundance) surpassing even that of the electron-capture case. Finally, it should be mentioned that fragmentation patterns in the case of direct ionization are rather similar to the recent electron impact ionization mass spectra obtained in [36,37].

Extension to other nucleobases, namely, adenine, cytosine, and thymine (Table I), shows that the branching ratio between the two ionization modes, EC and DI, as expressed for instance by the branching ratio EC:EC + DI, is rather similar for these nucleobases, i.e., having values at 80 keV proton energy of 27.1%, 27.6%, 26.6%, and 25.4% for adenine, cytosine, thymine, and uracil, respectively. These values are also close to the corresponding branching ratio measurements for gas-phase water, yielding 27.8% and 25.7% in two different studies [22,38]. The rather similar ratios for the nucleobases and water suggest that molecular details (for instance, the rather differing ionization energies which are important input parameters for the absolute cross sections) are not decisive for the relative probability of these two reactions.

Besides these details on fragmentation and differences concerning the ionization mechanisms, we are here also able to quantify the various reaction probabilities on an absolute scale. Figure 3 shows absolute cross sections in the energy

range from 20 to 150 keV for proton ionization of uracil, giving values for the total ionization cross sections and cross sections for those reactions proceeding via electron capture and those via direct ionization. Whereas the total cross section decreases in line with the Born-Bethe high-energy limit, the individual EC and DI contributions show different behavior, i.e., the EC cross section is strongly decreasing with increasing proton energy, whereas the DI cross section only decreases at higher energy approaching the Born-Bethe cross section. This leads to the situation that around the Bragg peak (20–150 keV) at 20 keV the branching ratios are about 60% and 40% for EC and DI, respectively; at around 35 keV, the two cross sections are equal; and at the highest energy studied here, at 150 keV, the branching ratios approach 10% for EC and 90% for DI. This behavior appears to be universal, as can be seen from Fig. 4 where the uracil branching ratio for EC as a function of energy is compared to a number of other targets, including H_2 [39] and some small molecules [22,38,39].

Finally, we are able here to report and compare experimental absolute cross-section values for a series of nucleobases.
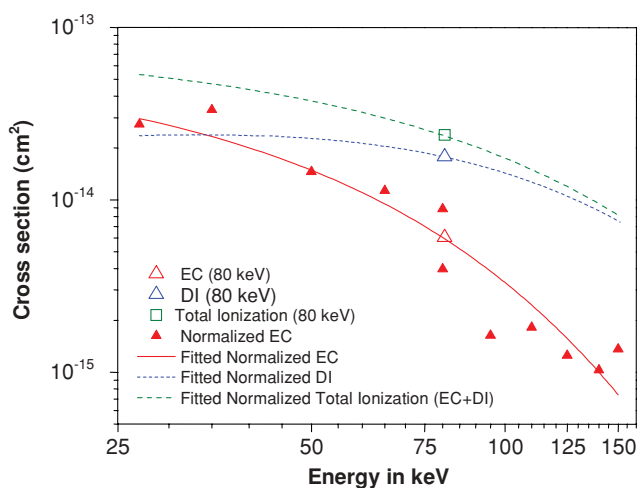

FIG. 3. (Color online) Absolute cross sections in the energy range from 20 to 150 keV for proton impact induced ionization of uracil including values for the total ionization cross sections and cross sections for those reactions proceeding via electron capture (EC) and those via direct ionization (DI).
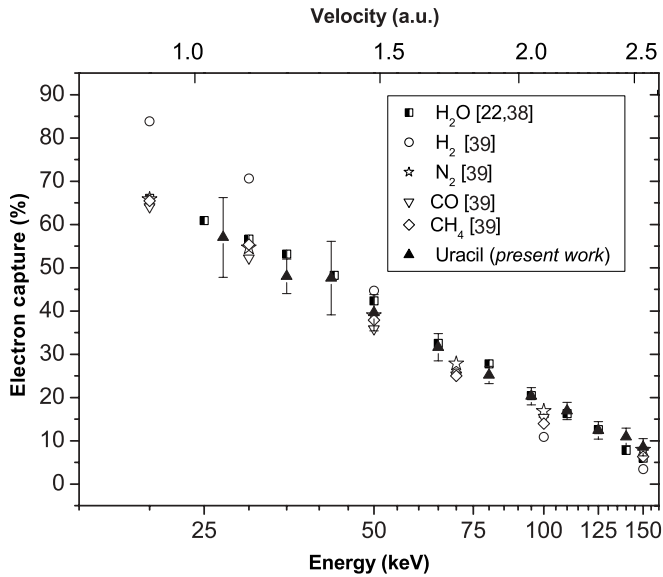
FIG. 4. Electron-capture ionization of uracil as a percentage of total ionization (electron capture + direct ionization) following proton impact in the energy range 27–150 keV. The data are compared to previous results for H_2O [22,38], and for H_2, N_2, CO, and CH_4 [39].

Table II gives cross-section values for 80 keV proton collisions with adenine, cytosine, thymine, and uracil. Surprisingly, while three of these nucleobases show rather similar values for the total, EC and DI cross sections, in contrast cytosine has in all three cases a cross section that is smaller by a factor of about 3.

A deeper insight into the details of this may be obtained by comparing these results with absolute electron impact ionization cross sections calculated recently [40,41] using the Deutsch-Märk (DM) and the Born and Bethe (BEB) methods, respectively. These semiclassical calculations take into account details of the electronic structure of the molecules under consideration and results obtained with DM and BEB agree in shape and magnitude. It is rather interesting to note that the maximum cross sections obtained in these calculations lie between 1.45 (uracil), 1.65 (cytosine), and 2.05 (adenine) $\times 10^{-15}$ cm^2. This is quite different in the ordering and different in magnitude from the present proton results, i.e., the direct-ionization cross sections for proton impact are about a factor of 4 (cytosine) to about 12 (uracil) larger than the electron-ionization cross sections. This tendency is in accordance with our earlier observations in water when comparing electron cross sections with direct-ionization cross sections taking into account the different projectile masses and comparing cross sections at the same velocities (see [22]

TABLE II. Absolute cross sections of electron capture, direct ionization, and total ionization in 80 keV proton collisions with gas-phase cytosine, uracil, thymine, and adenine.

Nucleobase	Cross section (10^{-15} cm^2)		
	EC	DI	Total
Cytosine (111 amu)	2.3 ± 0.5	6.0 ± 1.2	8.3 ± 1.6
Uracil (112 amu)	6.0 ± 1.2	17.7 ± 3.5	23.8 ± 4.8
Thymine (126 amu)	6.3 ± 1.3	17.3 ± 3.5	23.6 ± 4.7
Adenine (135 amu)	5.8 ± 1.2	15.5 ± 3.1	21.2 ± 4.2

and references therein) and has been attributed to target polarization effects. It was also argued that, at a fixed velocity, the lower kinetic energy of lighter projectiles reduces their cross sections relative to more massive counterparts as incident energy approaches the ionization potential of the target.

IV. CONCLUSION

In conclusion, we have presented here results based on an event-by-event analysis for the proton impact ionization of gas-phase nucleobases. This allows us to obtain a complete analysis in terms of the positive ions which are produced (and lost as in the case of reactions proceeding via electron capture by the proton). This experiment was possible after combining our high-energy-ion-beam–multicoincidence apparatus with a time-of-flight mass spectrometer operated in coincidence with the final projectile detection. A complete set of cross sections for the ionization of a target consisting of biologically relevant molecules (nucleobases) by proton impact has been obtained including the total and all partial cross sections and, in addition, differentiating between the direct-ionization and the electron-capture mechanisms. As this investigation yields a wealth of information on proton impact ionization, we are confident that such measurements will provide an important impact and basis for future refinement of the theoretical treatment of these reactions and their influence on radiation biology.

[1] E. W. McDaniel, J. B. A. Mitchell, and M. E. Rudd, *Atomic Collisions, Heavy Particle Projectiles* (Wiley, New York, 1993).

[2] See Proceedings of the Molecules of Biological Interest in the Gas Phase, Experimental Tools and Quantum Chemistry, Euresco Conference, Centre de Physique des Houches, France, 2000 (unpublished).

[3] L. Sanche, Eur. Phys. J. D **35**, 367 (2005).

[4] J. F. Ward, Radiat. Res. **104**, S103 (1985).

[5] P. Bernhardt, W. Friedland, P. Jacob, and H. G. Paretzke, Int. J. Mass Spectrom. **223**, 579 (2003).

[6] B. Boudaiffa, P. Cloutier, D. Hunting, M. A. Huels, and L. Sanche, Science **287**, 1658 (2000).

[7] G. Hanel, B. Gstir, S. Denifl, P. Scheier, M. Probst, B. Farizon, M. Farizon, E. Illenberger, and T. D. Mark, Phys. Rev. Lett. **90**, 188104 (2003).

[8] S. Ptasinska *et al.*, Angew. Chem. Int. Ed. **44**, 6941 (2005).

[9] P. Burrow *et al.*, J. Chem. Phys. **124**, 124310 (2006).

[10] S. Ptasinska *et al.*, Angew. Chem. Int. Ed. **45**, 1893 (2006).

[11] S. Denifl *et al.*, Angew. Chem. Int. Ed. **46**, 5238 (2007).

[12] S. Ptasinska *et al.*, Angew. Chem. Int. Ed. **44**, 1647 (2005).

[13] S. Ptasinska, S. Denifl, V. Grill, T. D. Mark, E. Illenberger, and P. Scheier, Phys. Rev. Lett. **95**, 093201 (2005).

[14] L. Sanche, Chem. Phys. Lett. **474**, 1 (2009).

[15] S. Martin, R. Bredy, A. R. Allouche, J. Bernard, A. Salmoun, B. Li, and L. Chen, Phys. Rev. A **77**, 062513 (2008).

[16] S. Bari *et al.*, J. Chem. Phys. **128**, 074306 (2008).

[17] S. Braccini, Nucl. Phys. B **172**, 8 (2007).

[18] H. Tawara and A. Russek, Rev. Mod. Phys. **45**, 178 (1973).

[19] L. H. Toburen, in *Atomic and Molecular Data for Radiotherapy and Radiation Research*, IAEA-TECDOC-799 (International Atomic Energy Agency, Vienna, 1995).

[20] H. Knudsen, U. Mikkelsen, K. Paludan, K. Kirsebom, S. P. Moller, E. Uggerhoj, J. Slevin, M. Charlton, and E. Morenzoni, J. Phys. B **28**, 3569 (1995).

[21] F. Gobet, B. Farizon, M. Farizon, M. J. Gaillard, M. Carré, M. Lezius, P. Scheier, and T. D. Märk, Phys. Rev. Lett. **86**, 3751 (2001).

[22] F. Gobet *et al.*, Phys. Rev. A **70**, 062716 (2004).

[23] F. Gobet *et al.*, Chem. Phys. Lett. **421**, 68 (2006).

[24] B. Coupier *et al.*, Eur. Phys. J. D **20**, 459 (2002).

[25] P. Moretto-Capelle and A. Le Padellec, Phys. Rev. A **74**, 062705 (2006).

[26] F. Alvarado, J. Bernard, B. Li, R. Bredy, L. Chen, R. Hoekstra, S. Martin, and T. Schlathölter, Chem. Phys. Chem. **9**, 1254 (2008).

[27] A. Le Padellec, P. Moretto-Capelle, M. Richard-Viard, J. P. Champeaux, and P. Carafelli, J. Phys. Conf. Ser. **101**, 012007 (2008).

[28] B. Farizon *et al.*, Int. J. Mass Spectrom. Ion Phys. **164**, 225 (1997).

[29] B. Farizon, M. Farizon, M. J. Gaillard, F. Gobet, M. Carre, J. P. Buchet, P. Scheier, and T. D. Märk, Phys. Rev. Lett. **81**, 4108 (1998).

[30] M. Carré, M. Druetta, M. L. Gaillard, H. H. Bukow, M. Horani, A. L. Roche, and M. Velghe, Mol. Phys. **40**, 1453 (1980).

[31] V. S. Troitskii, Sov. Phys. JETP **7**, 353 (1962).

[32] J. Tabet, S. Eden, S. Feil, H. Abdoul-Carime, B. Farizon, M. Farizon, S. Ouaskit, and T. D. Märk, Nucl. Instrum. Methods Phys. Res. B **268**, 2458 (2010).

[33] T. Schlathölter, F. Alvarado, and R. Hoekstra, Nucl. Instrum. Methods Phys. Res. B **233**, 62 (2005).

[34] J. Tabet, S. Eden, S. Feil, H. Abdoul-Carime, B. Farizon, M. Farizon, S. Ouaskit, and T. D. Märk, Phys. Rev. A **81**, 012711 (2010).

[35] J. Tabet, S. Eden, S. Feil, H. Abdoul-Carime, B. Farizon, M. Farizon, S. Ouaskit, and T. D. Märk, Int. J. Mass Spectrom. **292**, 53 (2010).

[36] S. Denifl, B. Sonnweber, G. Hanel, P. Scheier, and T. D. Märk, Int. J. Mass Spectrom. **238**, 47 (2004).

[37] M. Imhoff, Z. Deng, and M. Huels, Int. J. Mass Spectrom. **262**, 154 (2007).

[38] H. Luna *et al.*, Phys. Rev. A **75**, 042711 (2007).

[39] M. E. Rudd, R. D. DuBois, L. H. Toburen, C. A. Ratcliffe, and T. V. Goffe, Phys. Rev. A **28**, 3244 (1983).

[40] P. Bernhardt and H. G. Paretzke, Int. J. Mass Spectrom. **223**, 599 (2003).

[41] P. Mozejko and L. Sanche, Radiat. Environ. Biophys. **42**, 201 (2003).